Crystallization Behavior and Mechanical Properties of Polypropylene Copolymer by *In Situ* Copolymerization with a Nucleating Agent and/or Nano-Calcium Carbonate

Weiping Zhu,[1] Guangping Zhang,[2] Jianyong Yu,[2] Gance Dai[1]

[1]*Polymer Processing Lab, East China University of Science and Technology, Shanghai 200237, China*
[2]*College of Textiles, Donghua University, Shanghai 200051, China*

Received 3 December 2002; accepted 5 March 2003

ABSTRACT: The crystallization behavior of polypropylene (PP) copolymer obtained by *in situ* reactor copolymerization with or without a nucleating agent and/or nano-$CaCO_3$ particles was investigated both by thermal analysis and by polarized light microscopy. The Avrami model is successfully used to describe the crystallization kinetics of the studied copolymer. The results of the investigation show that a dramatic decrease of the half-time of crystallization $t_{1/2}$, as well as a significant increase of the overall crystallization rate, are observed in the presence of the nucleating agent. These effects are further promoted in the presence of the nano-$CaCO_3$ particles. The incorporation of the nucleating agent and nano-$CaCO_3$ particles into PP copolymer remarkably improved the mechanical properties and heat distortion temperature. © 2003 Wiley Periodicals, Inc. J Appl Polym Sci 91: 431–438, 2004

Key words: poly(propylene) (PP); copolymerization; nanocomposites; nucleation; crystallization

INTRODUCTION

The addition of ethylene–propylene rubber (EPR) or polyethylene (PE) to polypropylene (PP) may improve the poor impact strength of PP at low temperature. There are two ways of EPR addition to PP.[1–3] One way is to melt-compound EPR with PP.[4–7] The other way is to prepare PP and EPR blends by *in situ* reactor copolymerization of the monomers directly.[8–11] Random or block propylene copolymers with low ethylene content are commercially extremely important because they improve the toughness of PP. However, the introduction of the rubber microparticles usually decreases the stiffness of the polymer; meanwhile, the nucleation rate and overall crystallization rate will be depressed, which may affect the mechanical properties and molding cycle time.[4] For this reason, nucleating agents are usually used to increase the crystallization rate.[12–14] In addition, if nanoscale fillers are added to the impact-modified matrix and dispersed very well, the interfacial force between the polymer and the nanoscale fillers will be reinforced, thus promoting concurrently thermal and mechanical properties.[15]

PP nanocomposites were prepared by melt mixing PP with nanoscale fillers,[15–21] but it is still difficult to uniformly disperse the nanoscale fillers into the matrix. Recent advances in polymer/clay and polymer/silicate nanocomposite materials have inspired efforts to disperse montmorillonite-based fillers in PP.[22–26] The crystallization and morphology of melt blends and *in situ* copolymer of PP and EPR with or without nucleating agents have been studied.[12–14] In this study, the PP copolymer with low ethylene content was prepared by *in situ* copolymerization of PP and EPR with a nucleating agent and nanoscale calcium carbonate (nano-$CaCO_3$) added. The crystallization behavior, morphology, and mechanical properties of the PP copolymer were investigated.

Correspondence to: G.-p. Zhang (zgp12@msn.com).
Contract grant sponsor: SINOPEC Corp.

Journal of Applied Polymer Science, Vol. 91, 431–438 (2004)

EXPERIMENTAL

Materials preparation

NA9981, a nucleating agent, was prepared in our laboratory. The nano-$CaCO_3$ (50–70 nm) was supplied by the National Engineering Research Center of Ultrafine Powder, East China University of Science and Technology.

The PP copolymer was prepared in a 10-L stirred bed reactor with a catalyst chamber and a cocatalyst chamber, manufactured by Beijing Research Institute of Chemical Industry (BRICI). A syringe pump was used for feeding propylene and the monomer composition was controlled with the on-line gas chromatography and mass flow controller.

In the stirred bed reactor, about 2000 g of propylene was injected by syringe pump at 70°C at first, then the cocatalyst and external electron donor (CHDMS) in the chamber were introduced successively. The catalyst, the nucleating agent, and/or nano-$CaCO_3$ particles were introduced together with another 500 g of propylene. After 1 h, some volume of ethylene was introduced into the reactor successively through the mass flow controller and the polymerization was terminated after 1 h.

The neat PP copolymer was designated as sample O, the PP copolymer containing 0.1 wt % of the nucleating agent as sample A, and the PP copolymer containing 0.1 wt % of the nucleating agent and 1 wt % of nano-$CaCO_3$ particles as sample B. The powdery samples were melt-squeezed into films for the next analysis.

Thermal analysis

DSC analysis was conducted with a Perkin–Elmer Pyris 1 differential scanning calorimeter (Perkin Elmer Cetus Instruments, Norwalk, CT) operating under N_2 atmosphere. In an isothermal crystallization run, the following procedure was employed: a sample of about 5 mg was first heated to 200°C and kept at this temperature for 10 min to remove any nucleation sites; the sample was then rapidly cooled to the crystallization temperature T_c and maintained until the crystallization was completed. In a nonisothermal crystallization run, a sample of about 5 mg was first heated to 200°C and kept at this temperature for 10 min, and then the sample was cooled to 50°C at constant cooling rates.

The exothermic peaks obtained from DSC thermograms were integrated to compute the absolute crystallinity X_c, according to

$$X_c = \Delta H_c / \Delta H_f \quad (1)$$

where ΔH_c is the heat released during the crystallization process and ΔH_f is the heat of fusion of a perfect crystal taken as 209 J/g for polypropylene.[7]

The relative crystallinity (degree of the crystalline conversion at time t) is expressed as

$$X_t = \frac{\int_0^t (dH/dt)\, dt}{\int_0^\infty (dH/dt)\, dt} \quad (2)$$

where dH/dt is the heat evolution rate during the crystallization process, the first integral is the crystallization heat evolution at time t, and the second integral is the total crystallization heat at the termination of the crystallization.

Polarized light microscope observation

An Olympus BX51 (Tokyo, Japan) polarized light microscope (PLM) equipped with a THMSE 600 hot stage and a JVC TK-C1380 camera video was used for studying the nucleation and growth of spherulites in isothermal crystallization.

The following procedure was used: a thin film sample was sandwiched between microscope slides. The sample was heated to 200°C and kept at this temperature for 5 min to destroy any traces of crystal; the sample was then rapidly lowered to a prefixed T_c and allowed to crystallize isothermally, while photographs were taken automatically at appropriate time intervals.

Mechanical properties test

The mechanical behavior was investigated on samples obtained by injection molding. A molding temperature of 215°C was used; the pressure in the mold was 5.5 MPa. Tests were performed according to ASTM standard methods.

RESULTS AND DISCUSSION

Isothermal crystallization

The evolution of relative crystallinity for the neat PP copolymer (sample O) and PP copolymer containing the nucleating agent NA9981 and/or nano-$CaCO_3$ particles (sample A or B) is shown as a function of time in Figure 1. It can be seen that the crystallization kinetics of the neat or filled PP copolymer is strongly affected by the temperature. The PP copolymer containing NA9981 and/or nano-$CaCO_3$ particles crystallizes much faster than the neat PP copolymer at the same crystallization temperatures. This effect is still more evident in the evolution of the relative crystallinity isothermally crystallized at 139°C for three samples analyzed, which is represented in Figure 2.

This is ascribed to the differences in the crystallization processes for the neat and filled PP copolymer. The number of nuclei in samples A and B is much larger than that in sample O; thus, crystallization of the filled PP copolymer proceeds mainly by heterogeneous nucleation, whereas that of the neat PP copolymer proceeds both by heterogeneous and homogeneous nucleation mechanism. At higher crystallization temperatures it takes more time for homogeneous nucleation to start spontaneously by chain aggregation, whereas heterogeneous nuclei form simultaneously as soon as the sample reaches the crystallization temperature. The selected NA9981 is a type of crystalline organic phosphate nucleating agent, and its chemical structure has little effect on the copolymerization of the monomers. As a result, it acts only as a heterogeneous nucleating agent and increases the crystalliza-

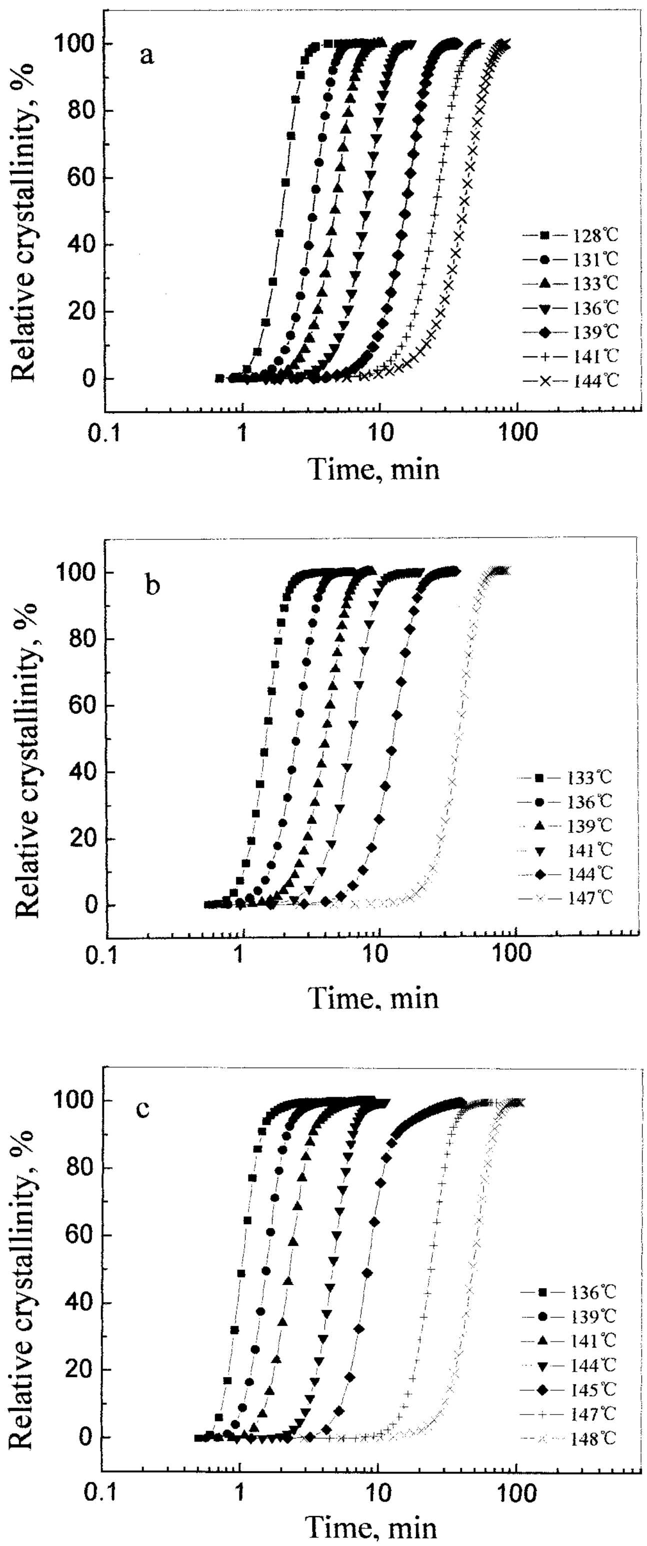

Figure 1 Changes of relative crystallinity for sample O (a) sample A (b) and sample B (c) as a function of time during isothermal crystallization.

tion rate of the polymer. Furthermore, the coexistence of only 1 wt % of nano-$CaCO_3$ particles in *in situ* copolymerization supplies much more nucleation sites and leads to a further increase of the crystallization rate of the PP copolymer. In general, the nucleation ability of the calcium carbonate particles is weak.[27] With the decrease of its size, the completion crystallization exotherm shifts to higher temperatures, showing higher nucleation effects.[21,28] The special performance of nano-$CaCO_3$ particles exhibits excellent nucleation ability and markedly improves other properties such as impact strength and flexural modulus, for example. However, the mechanism of interaction between nano-$CaCO_3$ particles and PP copolymer in the copolymerization process is subject to further investigation.

The evolution of the relative crystallinity under isothermal crystallization conditions can be described by an Avrami model[29,30]:

$$X_t = 1 - \exp(-kt^n) \tag{3}$$

where k is the rate constant, n is the Avrami exponent, and X_t is the crystalline conversion at time t. Hence the parameters of eq. (3), n and k, can be obtained from the plot of $\ln[-\ln(1 - X_t)]$ versus $\ln t$. The values of relative crystallinity lower than 50% were considered. These parameters are summarized in Table I for all samples. The rate constant decreases with increasing crystallization temperature T_c. Evidently, the crystallization takes place by a nucleation-controlled mechanism.

The Avrami exponent for sample O is in the range 2.8–3.0 at the crystallization temperatures studied. From these values of the Avrami exponents, it can be established that spherulitic development arises from an athermal and instantaneous nucleation. The Avrami exponent for sample A is in the range of 2.6–3.0. This means that the presence of the nucleating

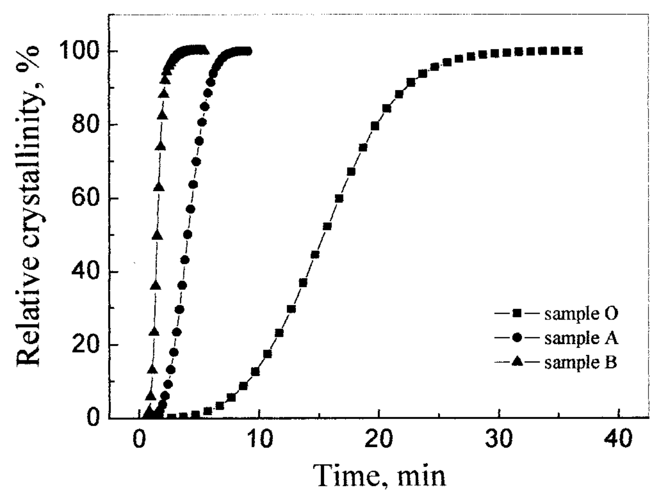

Figure 2 Comparison of the evolution of the relative crystallinity isothermally crystallized at 139°C for samples O, A and B.

TABLE I
Kinetic Parameters of Isothermal Crystallization for Samples O, A, and B

Material	T_c (°C)	n	K (min^{-n})	$t_{1/2}$ (min)	T_m (°C)
Sample O	128	2.8	3.44×1^{-1}	1.3	165.6
	131	2.9	5.28×1^{-2}	2.4	166.6
	133	2.9	1.34×1^{-2}	3.8	168.0
	136	3.0	2.00×1^{-3}	6.9	167.2
	139	3.0	2.69×1^{-4}	13.7	166.2
	141	2.9	6.76×1^{-5}	23.1	165.9
	144	2.7	3.14×1^{-5}	38.8	164.7
Sample A	133	2.6	8.02×1^{-1}	1.0	165.8
	136	2.8	1.20×1^{-1}	1.5	164.9
	139	2.8	2.30×1^{-2}	3.3	165.3
	141	2.9	5.54×1^{-3}	5.4	164.4
	144	3.0	5.40×1^{-4}	11.2	165.5
	147	2.9	4.10×1^{-5}	30.0	167.2
Sample B	136	2.6	3.77×1^{0}	0.5	167.1
	139	2.9	7.57×1^{-1}	1.0	166.7
	141	3.0	1.82×1^{-1}	1.5	167.9
	144	3.5	7.52×1^{-3}	3.6	169.1
	145	3.5	9.19×1^{-4}	6.7	170.9
	147	3.7	1.13×1^{-5}	20.3	172.1
	148	3.6	7.04×1^{-7}	44.5	173.2

agent does not change the mechanism of nucleation and crystal growth. The Avrami exponent for sample B is from 2.6 to 3.7, which is more dependent on temperature. These values suggests that at higher temperatures (e.g., >144°C) spherulitic development in the presence of nano-$CaCO_3$ particles arises from an athermal and random nucleation.

The half-time of crystallization $t_{1/2}$, defined as the time for 50% of the total crystallization to occur, can be read directly from Figure 1. The values of $t_{1/2}$ for all samples are also listed in Table I. With increasing the crystallization temperature, $t_{1/2}$ increases very rapidly, whereas the rate of crystallization decreases. For a given T_c, the $t_{1/2}$ value of the neat PP copolymer is significantly decreased in the presence of the nucleating agent, and is further decreased when nano-$CaCO_3$ particles are added together in copolymerization.

The crystallization rate is inversely related to $t_{1/2}$. A plot of $1/t_{1/2}$ versus T_c is shown in Figure 3. The crystallization rate of the PP copolymer containing the nucleating agent and nano-$CaCO_3$ at same crystallization temperatures is high. As can be seen, the temperature dependency of the crystallization kinetics for sample B is also high compared with that of the neat PP copolymer, which suggests that the number of the effective nuclei decreases more with decreasing the crystallization temperature. The nucleation activity and its temperature dependency are considered to be cooperative effects constituting many factors, including the physical and chemical nature of the agent as well as the interaction between the agent and the polymer.[31] The particular surface performance of nano-$CaCO_3$ particles may result in a different effect on the nucleation activity of the polymer.

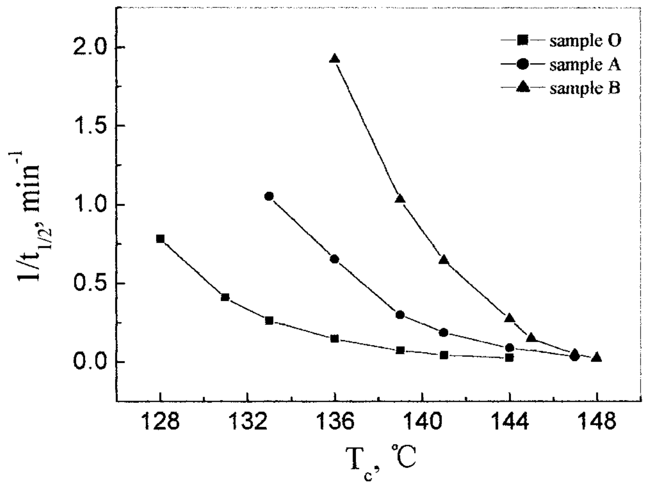

Figure 3 Variation of the reciprocal of the half-time of crystallization for samples O, A and B with the crystallization temperature.

The activation energy of isothermal crystallization can be determined according to the equation proposed by Cebe[32]:

$$k^{1/n} = k_0 \exp(-E/RT_c) \tag{4}$$

or

$$\text{Or} \quad \ln 1/t_{1/2} = \ln C - E/RT_c \tag{5}$$

where k_0 is a temperature-independent preexponential, E is the crystallization activation energy, R is the gas constant, and C is a constant. The plot of ln $t_{1/2}$ versus $1/T_c$ is shown in Figure 4. The activation energy magnitude was found to be 73 kcal mol^{-1} for crystallization of sample O, and 84 kcal mol^{-1} for

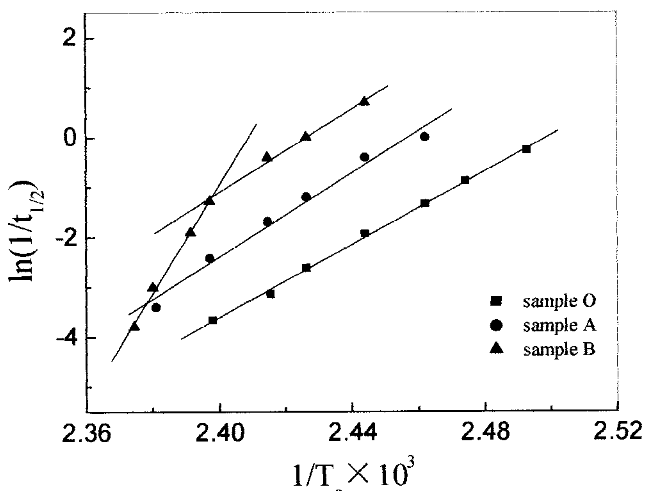

Figure 4 In($1/t_{1/2}$) vs. $1/T_c$ for determining the activation energy of isothermal crystallization of samples O, A and B.

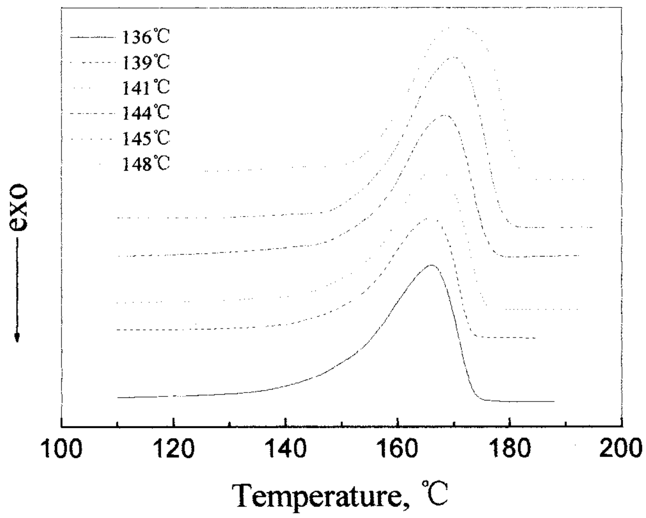

Figure 5 DSC scanning thermograms at 10 °C/min for sample B crystallizing at different crystallization temperatures.

crystallization of sample A. The addition of the nucleating agent in copolymerization process slightly increased the activation energy of crystallization of PP copolymer. At temperatures below 144°C, the activation energy of crystallization of sample B is 83 kcal mol^{-1}, which is the same as that of sample A. Above 144°C, however, its activation energy of crystallization rises to 214 kcal mol^{-1}, which suggests that the introduction of nano-$CaCO_3$ particles to PP copolymer leads to different mechanisms of nucleation and crystal growth at higher temperatures.

The effects of the crystallization temperature on the melting behavior of sample B are shown in Figure 5. Furthermore, melting temperatures of samples O and A, determined as the maximum of the endothermic peaks obtained in DSC scans of the isothermally crystallized samples, are also presented in Table I. The melting temperature increases slightly with the crystallization temperature, which is directly related to the polymer crystallite size. The incorporation of nano-$CaCO_3$ particles has only a slight effect on the values of the melting temperature. On the other hand, only the characteristic peak of α-spherulite polypropylene occurs in the crystallization and melting DSC thermograms, and that of the PE phase does not appear. The result suggests that the *in situ* copolymer synthesized possesses only a PP crystalline phase attributed to a low ethylene level. Moreover, no β-spherulite polypropylene is induced by nano-$CaCO_3$ particles, which is different from the results reported in the literature.[16,21,28]

Figure 6 shows the polarized light micrographs taken when the crystallization was completed for the neat PP copolymer and the PP copolymer with 0.1 wt % of NA9981 and/or 1 wt % of nano-$CaCO_3$ particles. The spherulitic size of the neat PP copolymer is greater than 40 μm and its spherulites are complete. Compared with pure isotactic PP, however, the spherulitic size of the neat PP copolymer is somewhat nonuniform, which is the result of the effect of EPR phase. The PP copolymer with the nucleating agent shows more spherulitic sites and a finer grainy morphology, whereas the PP copolymer with the nucleating agent and nano-$CaCO_3$ particles seems to exhibit the most dense and finest spherulites, and no spherulitic structure can be seen in PLM. In addition, upon cooling the melt to the same crystallization temperature, the nucleation rate of the nanocomposite is the most rapid of all three samples.

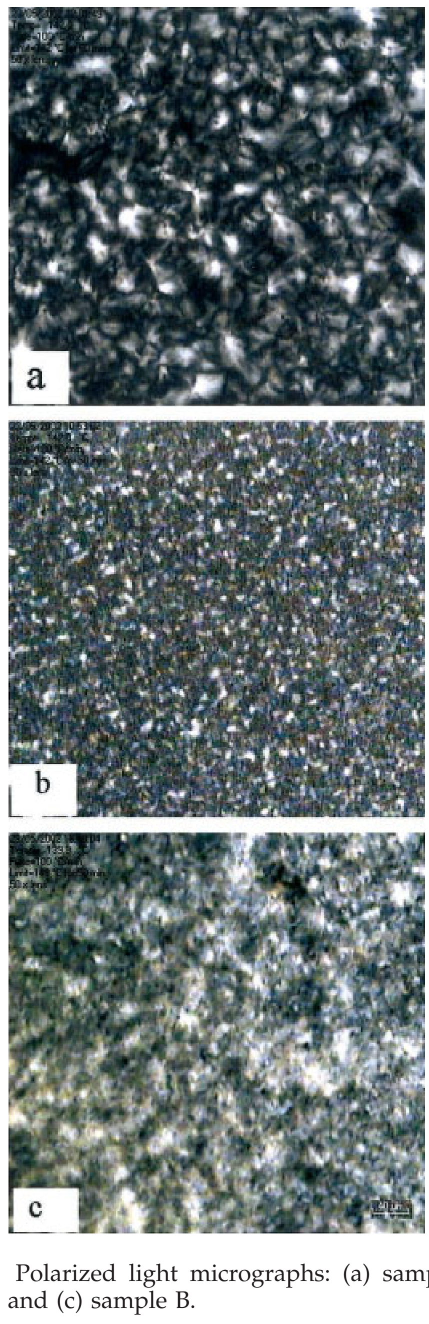

Figure 6 Polarized light micrographs: (a) sample O, (b) sample A and (c) sample B.

TABLE II
Various Parameters of Samples O, A, and B from DSC Nonisothermal Crystallization Exothermal Peaks

Material	Φ (°C/min)	T_c (°C)	T_{on} (°C)	T_m (°C)	X_c (%)
Sample O	3	127.5	130.9	166.2	34.6
	4	126.2	129.8	165.8	34.5
	5	124.8	128.7	166.2	33.1
	7.5	122.6	126.9	166.0	33.4
	10	120.3	124.5	164.6	32.7
	12.5	119.1	123.4	164.3	33.0
	15	117.8	122.4	164.6	32.1
	20	115.9	120.8	163.9	31.8
Sample A	3	132.9	136.5	166.2	32.1
	4	131.5	135.2	166.3	31.2
	5	130.2	134.1	165.6	32.0
	7.5	128.1	132.2	164.8	31.7
	10	126.7	130.7	164.8	31.7
	12.5	125.5	129.7	164.1	30.0
	15	124.3	128.8	164.2	30.8
	20	122.9	127.7	163.6	31.9
Sample B	3	138.1	140.4	167.3	36.7
	4	136.4	139.1	166.9	37.0
	5	135.4	138.4	167.4	36.8
	7.5	133.4	136.8	167.6	38.3
	10	132.2	135.8	167.0	37.4
	12.5	130.7	134.6	167.5	36.6
	15	129.6	133.9	167.8	35.7
	20	127.9	133.0	167.0	37.1

Nonisothermal crystallization

The effect of the nucleating agent and nano-$CaCO_3$ particles on the crystallization of the PP copolymer was also studied at different cooling rates (Φ). The absolute crystallinity (X_c), the apparent melting temperature (T_m), the crystallization peak temperature (T_c), and the onset temperature (T_{onset}), obtained from the DSC thermograms of nonisothermal crystallization, are given in Table II. The results show that both the additives and the cooling rate have a substantial effect on T_c and T_{onset}. In particular, T_c decreases as the cooling rate increases, whereas it increases when the additives are incorporated into the copolymer. The degree of conversion of the crystalline phase as a function of temperature for a DSC scan at 10°C/min for three samples studied is shown in Figure 7. It is evident that the crystallization peak temperature is enhanced for the PP copolymer containing the nucleating agent, and promoted much more by the addition of nano-$CaCO_3$ particles. This behavior confirms the strong nucleation ability of nano-$CaCO_3$ particles on PP copolymer crystallization and is in agreement with the results obtained in the isothermal analysis. Regarding the effect of the nucleating agent and nano-$CaCO_3$ particles on the melting temperature, no substantial differences were detected.

The effect of the nucleating agent and nano-$CaCO_3$ particles on the total absolute crystallinity of the PP copolymer is shown in Figure 8. A slight tendency to lower the total amount of crystallinity with the incorporation of the nucleating agent was observed. However, nano-$CaCO_3$ particles increased the absolute crystallinity of PP copolymer by about 10–20%. From the result of melt-compounding $CaCO_3$ nanoparticles with PP, Chan et al.[21] did not observe the change of crystallinity. The study by Rong et al.[17] showed that the addition of the untreated and polymer-grafted nanoparticles of SiO_2 (particle size of 7 nm) does not have a significant effect on the crystallinity of PP composites, using existing compounding techniques. Consequently, it can be speculated that the addition of nano-$CaCO_3$ particles in copolymerization may exhibit different interactions between the nanoparticles and the polymer, compared with the melt-compounding process.

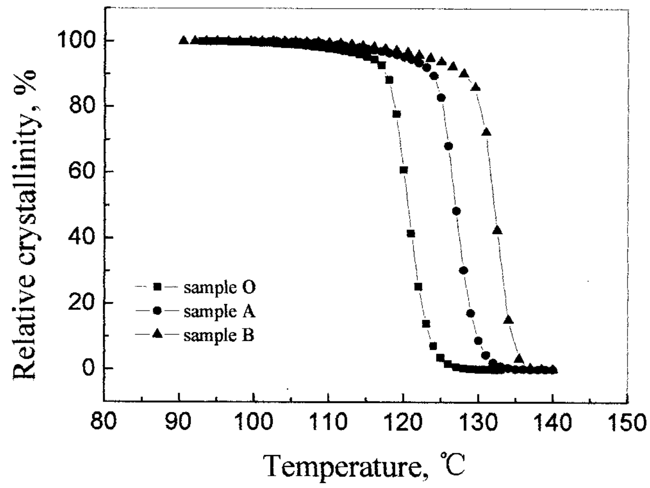

Figure 7 Nonisothermal crystallization curves of samples O, A and B scanning 10°C/min.

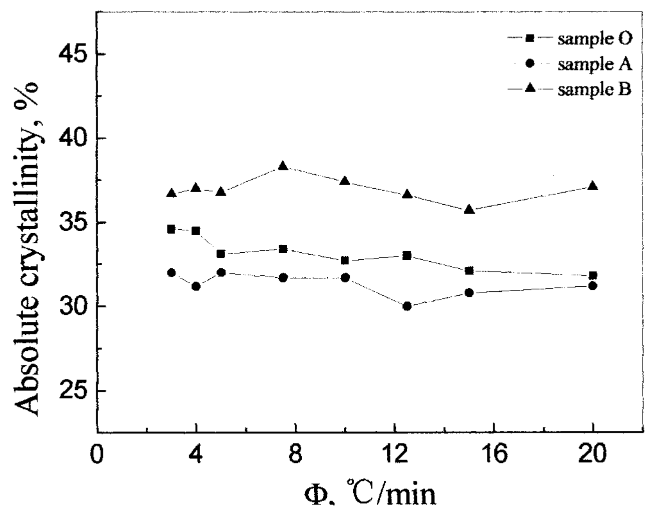

Figure 8 Comparison of absolute crystallinity for samples O, A and B at different cooling rates.

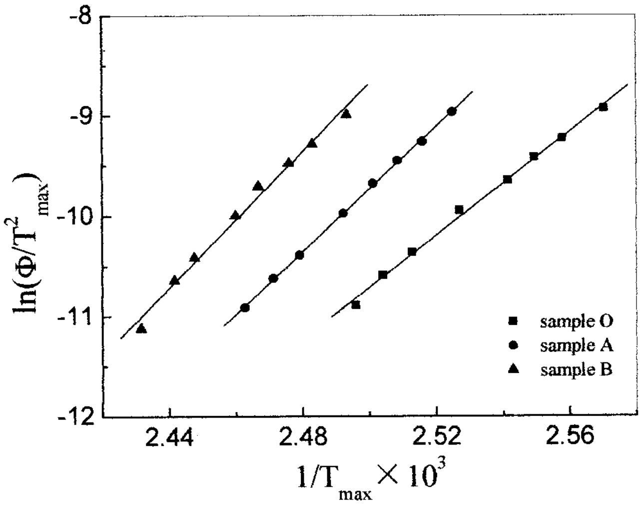

Figure 9 Evaluation of the nonisothermal crystallization activation energy for samples O, A and B by Kissinger method.

The activation energy of nonisothermal crystallization of PP copolymer can be determined by the Kissinger method[33]:

$$d(\ln(\Phi/T_{max}^2)/d(1/T_{max}) = -\Delta E/R \qquad (6)$$

where Φ is the cooling rate, $T_{\max}$ is the crystallization peak temperature, and R is the gas constant. Figure 9 shows the plot of $\ln(\Phi/T^2_{\max})$ against $1/T_{\max}$. According to the slope of the straight line, the activation energies of samples O, A, and B are determined as 51, 62, and 67 kcal/mol, respectively. These values are slightly lower than those calculated in the isothermal crystallization. It was found that the activation energy of nonisothermal crystallization of sample B does not change at all cooling rates, which means the mechanism of isothermal crystallization is different from that of the nonisothermal crystallization for the sample containing nano-$CaCO_3$ particles.

Mechanical properties

The mechanical properties of three samples are compared in Table III. Sample B shows a noticeable increase of mechanical properties, including flexural modulus (FM), notched impact strength (IS) at room or low temperature, as well as a higher heat distortion temperature (HDT), whereas sample A in the presence of the nucleating agent shows only a slight increase of mechanical properties and HDT. The enhancements of nano-$CaCO_3$ fillers are obvious even though the loading of nano-$CaCO_3$ is only 1%. That demonstrates the strong interaction between the nanoscale fillers and the polymer in copolymerization. As can be seen, PP systems conventionally filled (i.e., no nanoscale-level dispersion) by similar fillers, do not exhibit as large increase in their tensile modulus.[22] Similar improvements in mechanical properties can also be achieved by other layered particulate fillers; however, much higher filler loadings are required. For example, to obtain comparable tensile increases like those achieved by nanoscale montmorillonite dispersion (3 wt %), 30–60 wt % of talc or mica is needed.[34]

Generally speaking, the incorporation of inorganic fillers to polymers results in some loss of tensile strength with the increase of the filler loadings. However, the tensile results obtained by adding nano-$CaCO_3$ particles in this work are increased by 10%. As a result, it is possible to exhibit concurrent improvements in several materials properties through the introduction of low loadings of nano-$CaCO_3$ particles.

CONCLUSIONS

The crystallization of the neat PP copolymer and the PP copolymer by *in situ* copolymerization with the nucleating agent and/or nano-$CaCO_3$ particles follows Avrami behavior with the Avrami exponents of 2.8 to 3.0 for the neat PP copolymer, 2.6 to 3.0 for the PP copolymer in the presence of the nucleating agent, and 2.6 to 3.7 for the PP copolymer in the presence of the nucleating agent and nano-$CaCO_3$ particles. The addition of the nucleating agent and/or nano-$CaCO_3$ particles does not change the nucleation mechanism, but at higher crystallization temperatures, random nucleation seems to occur for the sample containing nano-$CaCO_3$ particles. The half-times of crystallization of these samples increases with increasing the crystallization temperature. The crystallization rate of the PP copolymer is significantly enhanced by the addition of the nucleating agent, and further promoted when nano-$CaCO_3$ particles are added together. However, the temperature dependency of the nucleation activity of PP copolymer/$CaCO_3$ nanocomposites is high compared with that of the neat sample. Moreover, the incorporation of nano-$CaCO_3$ particles into PP copolymer both forms much finer spherulites and increases the degree of crystallinity, thus significantly augmenting the flexural modulus and impact strength as well

TABLE III
Properties of the Neat and Filled PP Copolymers

Properly	Sample O	Sample A	Sample B
Loadings of NA9981, %	0	0.1	0.1
Loadings of $CaCO_3$, %	0	0	1.0
TS, MPa	33.0	35.6	36.3
Notched IS, J/m			
23°C	286	328	686
−23°C	20.6	23.3	31.0
FM, MPa	512	551	809
HDT, °C	69	71	91

as heat distortion temperature. The properties of PP copolymer are concurrently improved to a great extent by adding only 1 wt % nano-$CaCO_3$ particles in the *in situ* reactor copolymerization.

The authors acknowledge SINOPEC Corp. for financial support.

References

1. Moore, E. P. Polypropylene Handbook; Hanser: New York, 1996; pp 149–164.
2. Nomura, T.; Nishio, T.; Moriya, S.; Hashimoto, M. Kobunshi Ronbunshu 1994, 51, 569.
3. Nomura, T.; Nishio, T.; Sato, H.; Sano, H. Kobunshi Ronbunshu 1993, 50, 27.
4. Yokoyama, Y.; Ricco, T. J Appl Polym Sci 1997, 66, 1007.
5. Dorazio, L.; Mancarella, C.; Martuscelli, E.; Sticotti, G. Polymer 1993, 34, 3671.
6. Tribout, C.; Monasse, B.; Haudin, J. M. Colloid Polym Sci 1996, 274, 197.
7. Avalos, F.; Lopez-Manchado, M. A.; Arroyo, M. Polymer 1996, 37, 5681.
8. Galli, P.; Haylock, J. C.; Simonazzi, T. Polypropylene: Structures, Blends and Composites, Copolymers and Blends, Vol. 2; Karger-Kocsis, J., Ed.; Chapman & Hall: London, 1995; Chapter 1.
9. Nitta, K.; Kawada, T.; Yamahiro, M.; Mori, H.; Terano, M. Polymer 2000, 41, 6765.
10. Galli, P.; Haylock, J. C. Prog Polym Sci 1991, 16, 443.
11. Ito, J.; Mitani, K.; Mizutani, Y. J Appl Polym Sci 1992, 46, 1235.
12. Jang, G. S.; Cho, W. J.; Ha, C. S.; Kim, W.; Kim, H. K. Colloid Polym Sci 2002, 280, 424.
13. Zhang, R.; Zheng, H.; Lou, X.; Ma, D. J Appl Polym Sci 1994, 51, 51.
14. Zhang, R.; Lou, X.; Zheng, H.; Ma, D. Chem J Chinese Univ 1993, 10, 1464.
15. Wu, W.; Xu, Z. Acta Polymerica Sinica 2002, 1, 99.
16. Wang, X.; Huang, R. China Plastics 1999, 10, 22.
17. Rong, M.; Zhang, M.; Zheng, Y.; Walter, R.; Friedrich, K. Polymer 2001, 42, 167.
18. Calvert, P.; Burdon, J. Polym Mater Sci Eng 1994, 70, 224.
19. Kurokawa, Y.; Yasuda, H. J Mater Sci Lett 1996, 15, 1481.
20. Sumita, M.; Tsukumo, Y. J Mater Sci 1983, 18, 1758.
21. Chan, C. M.; Wu, J. S.; Li, J. X.; Cheung, Y. K. Polymer 2002, 43, 2981.
22. Manias, E.; Touny, A.; Wu, L.; Strawhecker, K.; Lu, B.; Chung, T. C. Chem Mater 2001, 13, 3516.
23. Kato, M.; Usuki, A.; Okada, A. J Appl Polym Sci 1997, 66, 1781.
24. Kawasumi, M.; Hasegawa, N.; Kato, M.; Usuki, A.; Okada, A. J Appl Polym. Sci 1998, 67, 87.
25. Tjong, S. C.; Meng, Y. Z.; Hay, A. S. Chem Mater 2002, 14, 44.
26. Manias, E.; Touny, A.; Wu, L.; Lu, B.; Strawhecker, K.; Gilman, J. W.; Chung, T. C. Polym Mater Sci Eng 2000, 82, 282.
27. Rybnikar, F. J Appl Polym Sci 1982, 27, 1479.
28. Fujiyama, M.; Wakino, T. J Appl Polym Sci 1991, 42, 2739.
29. Avrami, M. J Chem Phys 1939, 7, 1103.
30. Avrami, M. J Chem Phys 1940, 8, 212.
31. Kim, C. Y.; Kim, Y. C.; Kim, S. C. Polym Eng Sci 1993, 33, 1445.
32. Cebe, P.; Hong, S. Polymer 1986, 27, 1183.
33. Kissinger, H. E. J Res Natl Stds 1956, 57, 217.
34. Karian, H. G., Ed. Polypropylene: Structure, Blends and Composites; Marcel Dekker: New York, 1999.